

Orbit bifurcations and the scarring of wavefunctions*

J. P. Keating¹ and S. D. Prado²

1 School of Mathematics, University of Bristol, Bristol
BS8 1TW, UK, and BRIMS, Hewlett-Packard Laboratories,
Filton Road, Stoke Gifford, Bristol BS34 8QZ, UK.

2 Instituto de Física, Universidade Federal do Rio Grande do Sul
P.O. Box 15051, 91501-970 Porto Alegre, RS, Brazil.

December 2, 2024

Abstract

We extend the semiclassical theory of scarring of quantum eigenfunctions $\psi_n(\mathbf{q})$ by classical periodic orbits to include situations where these orbits undergo generic bifurcations. It is shown that $|\psi_n(\mathbf{q})|^2$, averaged locally with respect to position \mathbf{q} and the energy spectrum $\{E_n\}$, has structure around bifurcating periodic orbits with an amplitude and length-scale whose \hbar -dependence is determined by the bifurcation in question. Specifically, the amplitude scales as \hbar^α and the length-scale as \hbar^ω , and values of the *scar exponents*, α and ω , are computed for a variety of generic bifurcations. In each case, the scars are semiclassically wider than those associated with isolated and unstable periodic orbits; moreover, their amplitude is at least as large, and in most cases larger. In this sense, bifurcations may be said to give rise to *superscars*. The competition between the contributions from different bifurcations to determine the moments of the averaged eigenfunction amplitude is analysed. We argue that there is a resulting universal \hbar -scaling in the semiclassical asymptotics of these moments for irregular states in systems with a mixed phase-space dynamics. Finally, a number of these predictions are illustrated by numerical computations for a family of perturbed cat maps.

*Short title: Bifurcations and scarring

1 Introduction

One of the main goals in quantum chaology has been to determine the link between classical periodic orbits and quantum spectral fluctuations in the semiclassical limit. In fully chaotic systems, where the periodic orbits are isolated and unstable, this connection is embodied in Gutzwiller's trace formula (Gutzwiller 1971), and in integrable systems by a corresponding expression involving the phase-space tori (Berry & Tabor 1976). These formulae fail, by diverging, when periodic orbits bifurcate; that is, when combinations of stable and unstable orbits collide and transmute, or annihilate, as a system parameter varies – phenomena that characterize dynamics in the mixed regime. They must then be replaced by transitional or uniform approximations which interpolate through the bifurcation (Ozorio de Almeida & Hannay 1987; Tomsovic *et al.* 1995; Ullmo *et al.* 1996; Sieber 1996; Schomerus & Sieber 1997; Schomerus 1998; Sieber & Schomerus 1998).

That individual orbit bifurcations can have an important, and sometimes dominant influence on spectral statistics was pointed out by Berry *et al.* (1998), and demonstrated for a particular example, the perturbed cat maps. More generally, Berry *et al.* (2000) developed a semiclassical theory for the competition between the various generic bifurcations found in Hamiltonian systems to determine the moments of the quantum energy level counting function. This suggests that these moments diverge in a universal way, characterized by certain *twinkling exponents*, as $\hbar \rightarrow 0$.

A second major goal of quantum chaology has been to understand the influence of classical periodic orbits on quantum wavefunctions in the semiclassical limit. It was first noticed by McDonald (McDonald 1983) that individual eigenfunctions can have enhanced intensity along short periodic orbits in classically chaotic systems. This phenomenon was later studied systematically by Heller (Heller 1984), who called such structures *scars*. He developed a theory of scarring, based on wavepacket dynamics, which has subsequently been extended to describe a variety of statistical properties of quantum chaotic eigenfunctions (Kaplan 1999).

An alternative theory of scarring, based on an approach closely related to the trace formula, was initiated by Bogomolny (Bogomolny 1988). In this, the semiclassical approximation to the energy-dependent Green function is used to show that for quantum eigenfunctions $\psi_n(\mathbf{q})$ corresponding to energy levels E_n in a fixed energy range, $\langle |\psi_n(\mathbf{q})|^2 \rangle$, where $\langle \dots \rangle$ denotes an average over the states in question and locally over position \mathbf{q} , has complex-Gaussian fringes with, in two-degree-of-freedom systems, amplitude and length-scale of the order of $\hbar^{1/2}$ around unstable periodic orbits. A corresponding theory for Wigner functions was developed by Berry (1989).

We emphasize two limitations of the theories mentioned above. First, they only describe scarring in eigenfunctions that have been averaged over an energy interval which, semiclassically, contains a large number of states. Resummation techniques have been applied to provide some information about individual eigenfunctions (Agam & Fishman 1994; Fishman *et al.* 1996), but a detailed understanding of the phenomenon in this case remains to be developed. Second, they concentrate specifically on the influence of periodic orbits which are isolated and unstable. (Semiclassical theories describing the

connection between quantum wavefunctions and phase-space tori in classically integrable systems have also been developed; see, for example, Berry 1983 for a detailed review.)

Our purpose here is to address the second of these limitations. Specifically, our aim is to show how Bogomolny's theory can be extended to include the description of semiclassical structures in quantum eigenfunctions associated with generic classical periodic orbit bifurcations in systems with two degrees of freedom. We focus in particular on the \hbar -dependence of the amplitude and length-scale of the fringes corresponding to those identified by Bogomolny. Our main result is that the amplitude is of the order of \hbar^α , and the length-scale is of the order of \hbar^ω , where α and ω are bifurcation-dependent *scar exponents* whose values we calculate in a number of different cases. Crucially, $\omega > 1/2$ for all the bifurcations studied, and for most $\alpha > 1/2$ as well. In this sense, bifurcations may be said to give rise to *superscars*. In order to quantify this, we determine the way in which bifurcating orbits contribute, via a competition, to the semiclassical asymptotics of the moments of $\langle |\psi_n(\mathbf{q})|^2 \rangle$, in the same way as was done for spectral fluctuations by Berry *et al.* (2000). It is argued that this competition results in universal \hbar -scalings of the moments for the irregular eigenfunctions of systems with mixed phase-space dynamics. Finally, as an example, we apply some of the techniques developed to study the influence of one particular bifurcation on the eigenfunctions of a family of quantum perturbed cat maps.

2 Scar Formulae

Our aim in this section is to derive semiclassical scar formulae for bifurcating periodic orbits which generalize those obtained in Bogomolny (1988) for unstable orbits far from bifurcation.

We begin, following Bogomolny, with the energy-dependent Green function

$$G(\mathbf{q}', \mathbf{q}; E) = \sum_n \frac{\psi_n^*(\mathbf{q}') \psi_n(\mathbf{q})}{E - E_n}, \quad (1)$$

where $\psi_n(\mathbf{q})$ is the eigenfunction of the quantum Hamiltonian corresponding to the energy level E_n . The identity we seek to exploit follows from setting $\mathbf{q}' = \mathbf{q}$:

$$\sum_n |\psi_n(\mathbf{q})|^2 \delta_\varepsilon(E - E_n) = -\frac{1}{\pi} \text{Im} G(\mathbf{q}, \mathbf{q}; E + i\varepsilon). \quad (2)$$

Here, $\delta_\varepsilon(x)$ is a normalized, Lorentzian-smoothed δ -function of width ε . (It is straightforward to transform (2) to give differently smoothed δ -functions, for example Gaussians.) The left-hand side of (2) thus corresponds to a sum over eigenstates for which E_n lies within a range of size of the order of ε centred on E . Semiclassically, it is approximately the average of $|\psi_n(\mathbf{q})|^2$ with respect to these states multiplied by $\bar{d}(E)$, the mean level density. For systems with two-degrees-of-freedom

$$\bar{d}(E) \sim \frac{V(E)}{(2\pi\hbar)^2} \quad (3)$$

as $\hbar \rightarrow 0$, where

$$V(E) = \int \delta(E - H(\mathbf{p}, \mathbf{q})) d^2\mathbf{q} d^2\mathbf{p} \quad (4)$$

and $H(\mathbf{p}, \mathbf{q})$ is the classical Hamiltonian.

The connection with classical mechanics is achieved using the semiclassical approximation to the Green function. For systems with two-degrees-of-freedom, this is

$$G(\mathbf{q}', \mathbf{q}; E) \approx \frac{1}{i\hbar\sqrt{2\pi i\hbar}} \sum_{\gamma} \sqrt{|D_{\gamma}|} \exp \left\{ \frac{i}{\hbar} S_{\gamma}(\mathbf{q}', \mathbf{q}; E) - \frac{i\pi}{2} \nu_{\gamma} \right\}, \quad (5)$$

where the sum includes all classical trajectories from \mathbf{q} to \mathbf{q}' at energy E , S_{γ} is the action along the trajectory labelled γ ,

$$D_{\gamma} = \det \begin{pmatrix} \frac{\partial^2 S_{\gamma}}{\partial \mathbf{q}' \partial \mathbf{q}} & \frac{\partial^2 S_{\gamma}}{\partial \mathbf{q}' \partial E} \\ \frac{\partial^2 S_{\gamma}}{\partial E \partial \mathbf{q}} & \frac{\partial^2 S_{\gamma}}{\partial E^2} \end{pmatrix}, \quad (6)$$

and ν is the Maslov index (Gutzwiller 1990). When $\mathbf{q}' = \mathbf{q}$, the sum in (5) is clearly over closed orbits.

We note in passing that it follows from (2) that

$$\sum_n \delta_{\varepsilon}(E - E_n) = -\frac{1}{\pi} \operatorname{Im} \int G(\mathbf{q}, \mathbf{q}; E + i\varepsilon) d^2\mathbf{q}. \quad (7)$$

Substituting in the closed orbit sum for $G(\mathbf{q}, \mathbf{q}; E + i\varepsilon)$ and integrating term-by-term using the method of stationary phase leaves contributions from the periodic orbits. Assuming these are all isolated, as is the case for hyperbolic systems, the result is the trace formula (Gutzwiller 1971)

$$\sum_n \delta_{\varepsilon}(E - E_n) \approx \bar{d}(E) + \frac{1}{\pi\hbar} \sum_p \sum_{r=1}^{\infty} \frac{T_p}{\sqrt{|\det(\mathbf{M}_p^r - \mathbf{I})|}} \times \cos \left(\frac{rS_p}{\hbar} - r\nu_p \frac{\pi}{2} \right) \exp \left[-\varepsilon \frac{rT_p}{\hbar} \right], \quad (8)$$

where p labels primitive periodic orbits with period T_p and monodromy matrix \mathbf{M}_p , and r labels repetitions. As noted in the Introduction, this formula fails at bifurcations, where $\det(\mathbf{M}_p^r - \mathbf{I}) = 0$. Assuming that the periodic orbits lie in families which form tori in phase space gives the corresponding expression for integrable systems (Berry & Tabor 1976).

Bogomolny's scar formula follows not from integrating over all positions \mathbf{q} , as in (7), but from performing a *local average* of (2) with respect to \mathbf{q} (we postpone specifying the size of the averaging range until after the result has been stated), which we take to be smooth (convolution with a normalized Gaussian, for example). On the left-hand side this

gives, approximately, $\bar{d}(E) \langle |\psi_n(\mathbf{q})|^2 \rangle$, where $\langle \dots \rangle$ denotes a combination of the spectral average described above and the local \mathbf{q} -average. On the right-hand side, the \mathbf{q} -average selects from the closed orbits those that are close to periodic orbits (i.e. for which the change in momentum after return is appropriately small). These can then be described by linearizing about the periodic orbits. Essentially, this corresponds to expanding the action up to terms which are quadratic in the distance from the periodic orbit. The result is that

$$\sum_n \langle |\psi_n(\mathbf{q})|^2 \rangle_{\mathbf{q}} \delta_{\epsilon}(E - E_n) \approx \frac{1}{(2\pi\hbar)^2} \Omega(\mathbf{q}; E) - \frac{1}{\pi\hbar^{3/2}} \text{Im} \frac{1}{i\sqrt{2\pi i}} \sum_p \sum_{r=1}^{\infty} \frac{1}{|\dot{z}| \sqrt{[\mathbf{M}_p^r(z)]_{12}}} \times \exp \left[\frac{i}{\hbar} \left(rS_p + \frac{1}{2} \frac{\det(\mathbf{M}_p^r - I)}{[\mathbf{M}_p^r(z)]_{12}} y^2 - r\nu_p \frac{\pi}{2} \right) \right] \exp \left[-\varepsilon \frac{rT_p}{\hbar} \right], \quad (9)$$

where z is a coordinate along a given periodic orbit and y is a coordinate transverse to it, $[\mathbf{M}_p^r(z)]_{ij}$ denotes the elements of the monodromy matrix (which are functions of z), \dot{z} is the velocity along the periodic orbit, and

$$\Omega(\mathbf{q}; E) = \int \delta(E - H(\mathbf{p}, \mathbf{q})) d^2\mathbf{p}. \quad (10)$$

This in turn implies that

$$\langle |\psi_n(\mathbf{q})|^2 \rangle \approx \frac{\Omega(\mathbf{q}; E)}{V(E)} - \frac{4\pi\sqrt{\hbar}}{V(E)} \text{Im} \frac{1}{i\sqrt{2\pi i}} \sum_p \sum_{r=1}^{\infty} \frac{1}{|\dot{z}| \sqrt{[\mathbf{M}_p^r(z)]_{12}}} \times \exp \left[\frac{i}{\hbar} \left(rS_p + \frac{1}{2} \frac{\det(\mathbf{M}_p^r - \mathbf{I})}{[\mathbf{M}_p^r(z)]_{12}} y^2 - r\nu_p \frac{\pi}{2} \right) \right] \exp \left[-\varepsilon \frac{rT_p}{\hbar} \right]. \quad (11)$$

Equation (11) is Bogomolny's scar formula. In classically ergodic systems, the first term represents the quantum-ergodic limit of the eigenfunction probability density (Shnirelman 1974, Colin de Verdière 1985, Zelditch 1987). The second describes complex Gaussian fringes (the y -dependent part), with length-scale and amplitude both of the order of $\hbar^{1/2}$, associated with each periodic orbit. This structure will be resolved if the local \mathbf{q} -average is over regions whose dimensions are small compared to the length-scale of the fringes; that is, over regions whose dimensions scale as \hbar^{δ} , where $\delta > 1/2$. In order for the near-to-periodic-orbit approximation to be valid, we must also have $\delta < 1$; that is, the dimensions of the averaging range must be large compared to a de Broglie wavelength.

The trace formula (8) can be recovered from (9) by integrating over z and y . The z -integral gives the period in the amplitude of the periodic orbit contributions, and the y -integral gives the determinant. Note that the power of \hbar in the trace formula amplitude is the amplitude exponent in (9), $-3/2$ (which in turn is equal to the amplitude exponent in (11) minus two – the exponent in \bar{d}), plus the length-scale exponent of the fringes, $1/2$.

The approximations (9) and (11) break down in two ways. First, at self-focal points along an orbit $[\mathbf{M}_p^r(z)]_{12} = 0$ and the amplitude diverges. This can be remedied straightforwardly using Maslov's method, and we will not concern ourselves further with it here. Second, when an orbit bifurcates $\det(\mathbf{M}_p^r - \mathbf{I}) = 0$, and so the formulae become y -independent. Essentially, this means that the fringes are infinitely wide (it is this infinity which, upon integration with respect to y , transfers itself to the amplitude in the trace formula). Our purpose in this paper is to show how to correct (9) and (11) in this case.

It might be thought that the scar formulae for bifurcating orbits could be obtained easily by expanding the action in (5) to higher order than quadratic. For some of the simpler bifurcations (e.g. the codimension-one bifurcations of orbits with $r = 1$ and $r = 2$) this is correct (see the example in Section 4). However, for more complicated bifurcations it is incorrect, because for these the linearized map \mathbf{M}_p^r is equal to the identity, which cannot be generated by the action $S(\mathbf{q}', \mathbf{q}; E)$. Thus it is difficult to build into the semiclassical expression for the $\mathbf{q}\mathbf{q}'$ -representation of the Green function a well-behaved description of the nonlinear dynamics which the linearized map approximates. The solution to this problem, originally proposed in Ozorio de Almeida & Hannay (1987), is to transform the Green function to a mixed position-momentum representation, and this is the approach we now take.

The Ozorio de Almeida-Hannay method involves, first, Fourier transforming $G(\mathbf{q}', \mathbf{q}; E)$ with respect to \mathbf{q}' . This gives the Green function in the $\mathbf{q} \mathbf{p}'$ -representation, $\tilde{G}(\mathbf{p}', \mathbf{q}; E)$ (\mathbf{p}' is the momentum conjugate to \mathbf{q}'). The semiclassical approximation to \tilde{G} takes the same form as (5), except that $S(\mathbf{q}', \mathbf{q}; E)$ is replaced by the $\mathbf{q} \mathbf{p}'$ -generating function $\tilde{S}(\mathbf{p}', \mathbf{q}; E)$. $G(\mathbf{q}', \mathbf{q}; E)$ may then be rewritten, semiclassically, as the Fourier transform of this expression with respect to \mathbf{p}' . (For an alternative approach leading to the same final answer, see Sieber 1996). The result, for the semiclassical contribution to $G(\mathbf{q}, \mathbf{q}; E)$ from closed orbits in the neighbourhood of a bifurcating periodic orbit, takes the following form.

Consider the case of a codimension- K bifurcation of a periodic orbit with repetition number r . As before, let z be a coordinate along the orbit at bifurcation, let y be a coordinate transverse to it, and let p_y be the momentum conjugate to y , so that y and p_y are local surface of section coordinates. Let $\Phi_{r,K}(y, p_y, \mathbf{x})$ be the normal form which corresponds to the local (reduced) generating function in the neighbourhood of the bifurcation (Arnold 1978; Ozorio de Almeida 1988), where $\mathbf{x} = (x_1, x_2, \dots, x_K)$ are parameters controlling the unfolding of the bifurcation. Then, up to irrelevant factors, the contribution to $G(\mathbf{q}, \mathbf{q}; E)$ is

$$G_{r,K}(y; \mathbf{x}) = \frac{1}{\hbar^2} \int \exp \left[\frac{i}{\hbar} \Phi_{r,K}(y, p_y, \mathbf{x}) \right] dp_y \quad (12)$$

(as already stated, we are here interested in determining the \hbar -dependence of the amplitude and length-scale of the associated fringes, and so have neglected terms in (12), such as an \hbar -independent factor in the integrand, which do not influence these).

Before proceeding further, we make three remarks about (12). First, the power of \hbar outside the exponential arises from adding 1/2, which comes from the Fourier transform, to the exponent in (5), 3/2. Second, the representation used in Berry *et al.* (2000) for

the fluctuating part of the spectral counting function may be derived from (12) by taking the trace of $G_{r,K}$, which involves integrating the right-hand side of (12) with respect to y (the z -integral is trivial, as before), and then integrating with respect to E resulting in a further multiplication by \hbar . Likewise, the formulae of Ozorio de Almeida and Hannay (1987) correspond to taking the trace of $G_{r,K}$, keeping the terms we have neglected. Third, the \hbar -dependence of the fringes in Bogomolny's scar formula for unstable periodic orbits far from bifurcation can be recovered using the appropriate normal form:

$$\Phi_{r,0} = p_y^2 + y^2, \quad (13)$$

which corresponds to a particular, \hbar -independent choice of units for p_y and y . Evaluating the integral then gives

$$G_{r,0}(\mathbf{q}) \propto \frac{1}{\hbar^{3/2}} \exp\left(i \frac{y^2}{\hbar}\right), \quad (14)$$

as in (9).

Equation (12) is the starting point for the analysis of bifurcating orbits. Our strategy is essentially the same as that used in Berry *et al.* (2000) to study the related fluctuations in the spectral counting function (see also Berry 2000 for a review of applications to other areas in wave physics): first, rescale y and p_y to remove the $1/\hbar$ factor from the dominant term (germ) of $\Phi_{r,K}$ in the exponent, and then apply a compensating rescaling of the parameters x_1, x_2, \dots, x_K to remove the \hbar -dependence from the other terms which do not vanish as $\hbar \rightarrow 0$. This will lead to

$$G_{r,K}(y; \mathbf{x}; \hbar) = \frac{1}{\hbar^{2-\alpha_{r,K}}} G_{r,K}\left(\frac{y}{\hbar^{\omega_{r,K}}}, \left\{\frac{x_n}{\hbar^{\sigma_{n,r,K}}}\right\}, 1\right). \quad (15)$$

The exponent α describes the semiclassical amplitude of the fringes in $\langle |\psi_n(\mathbf{q})|^2 \rangle$ associated with the bifurcation, and the exponent ω describes the \hbar -dependence of their length-scale, or width. We call these the *scar exponents*. Note that the corresponding amplitude exponent in $\sum_n \langle |\psi_n(\mathbf{q})|^2 \rangle_q \delta_\varepsilon(E - E_n)$ is $2 - \alpha$. The exponents σ describe the range of influence of the bifurcation in the different unfolding directions x_n . Their sum

$$\gamma_{r,K} = \sum_{n=1}^K \sigma_{n,r,K} \quad (16)$$

describes the \hbar -scaling of the K -dimensional \mathbf{x} -space hypervolume affected by the bifurcation.

We now calculate these exponents in a variety of examples. Consider first the $r = 1$ bifurcations which correspond to cuspoid (i.e. corank 1) catastrophes. For these, the normal forms are (Berry *et al.* 2000)

$$\Phi_{1,K}(y, p_y; \mathbf{x}) = p_y^2 + y^{K+2} + \sum_{n=1}^K x_n y^n. \quad (17)$$

Substituting this into (12) and evaluating the integral then gives

$$G_{1,K}(y; \mathbf{x}) \propto \frac{1}{\hbar^{3/2}} \exp \left[\frac{i}{\hbar} \left(y^{K+2} + \sum_{n=1}^K x_n y^n \right) \right] \quad (18)$$

Making the rescalings $\tilde{y} = y/\hbar^{1/(K+2)}$, $\tilde{x}_n = x_n/\hbar^{1-n/(K+2)}$ removes the \hbar -dependence of the exponent, and so for the cuspoids we have

$$\alpha_{1,K} = \frac{1}{2}, \quad \omega_{1,K} = \frac{1}{K+2}, \quad \sigma_{n,1,K} = 1 - \frac{n}{K+1} \quad (19)$$

and

$$\gamma_{1,K} = \frac{K(K+3)}{2(K+2)}. \quad (20)$$

Analogous expressions can be written down for the $r = 1$ bifurcations corresponding to the more complicated case of catastrophes of corank 2 (see, for example, Berry 2000) in the same way.

When $r > 1$, the generic bifurcations with $K = 1$ have been classified by Meyer (Meyer 1970, 1986; Arnold 1978; Ozorio de Almeida 1988), and those with $K = 2$ by Schomerus (1998). The relevant parts of the corresponding normal forms, taken from Berry (2000) (to which readers are referred for further details), are summarized in Table 1 (in the expressions given, we are retaining only those terms which affect the exponents we seek to calculate).

r	$\Phi_{r,2}$
2	$p_y^2 + y^6 + x_1 y^2 + x_2 y^4$
3	$(p_y^2 + y^2)^2 + x_1(p_y^2 + y^2) + x_2 \operatorname{Re}[(p_y + iy)^3]$
4	$p_y^2 y^2 + x_1(p_y^2 + y^2) + x_2(p_y^2 - y^2)^2$
5	$\operatorname{Re}[(p_y + iy)^5] + x_1(p_y^2 + y^2) + x_2(p_y^2 + y^2)^2$
≥ 6	$(p_y^2 + y^2)^3 + x_1(p_y^2 + y^2) + x_2(p_y^2 + y^2)^2$

Table 1: The relevant parts of the normal forms for $K = 2$ bifurcations of period- r orbits (taken from Berry 2000). The corresponding expressions for $K = 1$ bifurcations, $\Phi_{r,1}$, follow from settling $x_2 = 1$.

The corresponding scar exponents, and the hypervolume exponents γ are given in Table 2 ($K = 1$) and Table 3 ($K = 2$).

Finally, we consider bifurcations of orbits for which $r \geq 2K + 2$. In this case, the relevant terms in the normal forms are (Berry *et al.* 2000)

$$\Phi_{r,K}(y, p_y; \mathbf{x}) = I^{K+1} + \sum_{n=1}^K x_n I^n + \mathcal{O}(I^{K+2}), \quad (21)$$

r	$\alpha_{r,1}$	$\omega_{r,1}$	$\gamma_{r,1}$
2	1/2	1/4	1/2
3	1/3	1/3	1/3
≥ 4	1/4	1/4	1/2

Table 2: Scar exponents for generic, codimension-1 bifurcations.

r	$\alpha_{r,2}$	$\omega_{r,2}$	$\gamma_{r,2}$
2	1/2	1/6	1
3	1/4	1/4	3/4
4	1/4	1/4	1/2
5	1/5	1/5	4/5
≥ 6	1/6	1/6	1

Table 3: Scar exponents for generic, codimension-2 bifurcations.

where

$$I = y^2 + p_y^2. \quad (22)$$

Expressing Φ in terms of y and p_y , we find

$$\alpha_{r,K} = \omega_{r,K} = \frac{1}{2(K+1)} \quad (23)$$

and

$$\gamma_{r,K} = \frac{K}{2} \quad (24)$$

(c.f. the $r \geq 4$ exponents in Table 2, and the $r \geq 6$ exponents in Table 3).

The main point we wish to draw attention to is that, in all the cases listed above, $\omega < 1/2$ and $\alpha \leq 1/2$, and that in most cases $\alpha < 1/2$. Recall that $\omega = \alpha = 1/2$ for periodic orbits far from bifurcation. In this sense, bifurcations may be said to give rise to *superscars*; that is, to scars that are semiclassically wider, and often greater in amplitude than those associated with non-bifurcating orbits. We shall demonstrate this with an explicit example in Section 4.

The width exponent ω determines the scale for the \mathbf{q} -average in $\langle |\psi_n(\mathbf{q})|^2 \rangle$ which allows the fringe structure to be resolved. Specifically, if the dimensions of the averaging range scale semiclassically as \hbar^δ , the fringe structure will be resolved if $\delta > \omega$, but not if $\delta < \omega$. Recall that for the approximation to hold in which the main contribution to the average comes from closed orbits in the neighbourhood of periodic orbits, we must also have $\delta < 1$; that is, the average must extend over many de Broglie wavelengths.

We also note that the scar exponents satisfy

$$\beta = 1 - \alpha - \omega, \quad (25)$$

where β is the amplitude exponent of the fluctuations in the spectral counting function associated with the bifurcation in question (Berry *et al.* 2000). This follows from a comparison of (12) with the corresponding expression for the counting function, which, as already noted, corresponds to integrating (12) with respect to y and multiplying by \hbar . It generalizes the connection discussed above between the power of \hbar in the trace formula for $d(E)$ and the amplitude and width exponents of Bogomolny's fringes for non-bifurcating orbits.

3 Moment asymptotics

One way to quantify scarring effects is in terms of the moments of the wavefunctions. Consider the case when all periodic orbits are isolated and unstable. We define

$$C_{2m}(\hbar) = \frac{1}{\Delta q} \int \left(\left\langle |\psi_n(\mathbf{q}')|^2 \right\rangle - \frac{\Omega(\mathbf{q}'; E)}{V(E)} \right)^{2m} d^2 \mathbf{q}' \quad (26)$$

where the \mathbf{q}' -integral is over an \hbar -independent volume Δq . Note that these are the moments not of the amplitude of the wavefunction itself, but of the amplitude averaged with respect to position (over a region which shrinks as $\hbar \rightarrow 0$, but which contains an increasing number of de Broglie wavelengths) and energy (semiclassically many levels).

Assuming that the wavefunctions are quantum ergodic on the scale of the local \mathbf{q} -average implies that $C_{2m}(\hbar) \rightarrow 0$ as $\hbar \rightarrow 0$ when $m > 0$. It follows from the fact that the fringes in (11) have scar exponents $\alpha = \omega = 1/2$ that their individual contributions to the moments scale as $\hbar^{m+1/2}$ in this limit. The corresponding contribution from a bifurcating orbit is of the order of $\hbar^{2m\alpha+\omega}$, and so is semiclassically larger. For the bifurcations of periodic orbits with $r = 1$ corresponding to the cuspid catastrophes we have that

$$\tilde{\mu}_{m,1,K} = 2m\alpha_{1,K} + \omega_{1,K} = m + \frac{1}{K+2}. \quad (27)$$

The values of these exponents for the generic bifurcations with $K = 1$ and $K = 2$ when $r > 1$ are given in Table 4 and Table 5, for $m \leq 3$.

r	$\tilde{\mu}_{1,r,1}$	$\bar{\mu}_{1,r,1}$	$\tilde{\mu}_{2,r,1}$	$\bar{\mu}_{2,r,1}$	$\tilde{\mu}_{3,r,1}$	$\bar{\mu}_{3,r,1}$
2	5/4	7/4	9/4	11/4	13/4	15/4
3	1	4/3	5/3	6/3	7/3	8/3
≥ 4	3/4	5/4	5/4	7/4	7/4	9/4

Table 4: Values of $\tilde{\mu}_{m,r,1} = 2m\alpha_{r,1} + \omega_{r,1}$ and $\bar{\mu}_{m,r,1} = 2m\alpha_{r,1} + \omega_{r,1} + \gamma_{r,1}$ for the codimension-1 scar exponents listed in Table 2.

The moments defined by (26) are implicitly functions of the system parameters \mathbf{x} . Averaging them with respect to \mathbf{x} produces an opportunity for a competition between the various generic bifurcations. The contribution of each bifurcation must be weighted

r	$\tilde{\mu}_{1,r,2}$	$\bar{\mu}_{1,r,2}$	$\tilde{\mu}_{2,r,2}$	$\bar{\mu}_{2,r,2}$	$\tilde{\mu}_{3,r,2}$	$\bar{\mu}_{3,r,2}$
2	7/6	13/6	13/6	19/6	19/6	25/6
3	3/4	3/2	5/4	2	7/4	5/2
4	3/4	5/4	5/4	7/4	7/4	9/4
5	3/5	7/5	1	9/5	7/5	11/5
≥ 6	1/2	3/2	5/6	11/6	7/6	13/6

Table 5: Values of $\tilde{\mu}_{m,r,2} = 2m\alpha_{r,2} + \omega_{r,2}$ and $\bar{\mu}_{m,r,2} = 2m\alpha_{r,2} + \omega_{r,2} + \gamma_{r,2}$ for the codimension-2 scar exponents listed in Table 3.

by the associated hypervolume in \mathbf{x} -space, and so scales as $\hbar^{2m\alpha+\omega+\gamma}$, provided that the \mathbf{x} -average of the $2m$ th power of the \hbar -independent term in (15) exists (see Berry 1977 for a discussion of this subtle point). For the $r = 1$ bifurcations corresponding to the cuspoid catastrophes,

$$\bar{\mu}_{m,1,K} = 2m\alpha_{1,K} + \omega_{1,K} + \gamma_{1,K} = m + \frac{K+1}{2}. \quad (28)$$

When $r > 1$, the values of these exponents for the generic bifurcations with $K = 1$ and $K = 2$ are also listed in Table 4 and Table 5. The bifurcation that wins the competition, and hence which determines the rate at which the \mathbf{x} -averaged moments tend to zero in the semiclassical limit, is the one for which $2m\alpha + \omega + \gamma$ is minimized; that is,

$$\frac{1}{\hbar^{\mu_m}} \langle C_{2m}(\hbar) \rangle_{\mathbf{x}} = o(\hbar^\epsilon) \quad (29)$$

for any $\epsilon < 0$, with

$$\mu_m = \min(2m\alpha + \omega + \gamma) \quad (30)$$

where $\langle C_{2m}(\hbar) \rangle_{\mathbf{x}}$ denotes the \mathbf{x} -averaged moments and the minimum is with respect to the generic bifurcations. This, of course, assumes that the minimum exists. We now argue that it does.

Our reasoning is based directly on that of Berry *et al.* (2000), where the analogous problem of the moments of fluctuations in the level counting function was considered. First, we note that if the competition is restricted to bifurcations with $r \geq 2K + 2$, then

$$\min(2m\alpha + \omega + \gamma) = \min_K \left(\frac{2m+1}{2(K+1)} + \frac{K}{2} \right), \quad (31)$$

which exists for any m and can be calculated straightforwardly. Second, it was shown by Berry *et al.* that each bifurcation with $r \geq 2K + 2$ has a counterpart with $r < 2K + 2$ with the property that the counterpart has a normal form with the same germ, and so the same α and ω exponents, but a larger γ exponent. Hence (31) represents the minimum with respect to all of the generic bifurcations and so

$$\mu_m = \min_K \left(\frac{2m+1}{2(K+1)} + \frac{K}{2} \right). \quad (32)$$

For example, $\mu_1 = 5/4$ (coming from $K = 1$), $\mu_2 = 7/4$ (also coming from $K = 1$), and $\mu_3 = 13/6$ ($K = 2$). In general $\mu_m \approx \sqrt{2m+1} - 1/2$.

It is natural to compare μ_m to the corresponding exponent for Gaussian random functions, which are often taken as models of quantum chaotic wavefunctions. In that case, the moments (26) are semiclassically of the order of \hbar^m . This follows from the results of Section IIIB of Eckhardt *et al.* 1995, if the operator considered there is the characteristic function of the region over which the local \mathbf{q} -average in (26) extends. The same rate of vanishing also holds for the eigenvectors of random hermitian matrices (see Section IIIA of Eckhardt *et al.*). (Readers are referred to Bäcker *et al.* 1998 for a detailed review of the rate of quantum ergodicity, and its characterization by moments analogous to those defined by (26)). Crucially, we note that $\mu_m \leq m$ for $m > 1$, and so then, if the background to the scars due to individual periodic orbits is modelled by a Gaussian random function, bifurcations dominate the semiclassical asymptotics. The contributions from individual non-bifurcating orbits are always subdominant.

To summarize, the exponents μ_m , which are analogous to the *twinkling exponents* of Berry *et al* (2000), determine the asymptotic scaling of the parameter-averaged moments C_{2m} in the limit as $\hbar \rightarrow 0$ when $m > 1$. Note that they are universal, that is, system independent. Note also that they are determined solely by generic bifurcation processes. As pointed out in the Introduction, these processes are characteristic of mixed phase-space dynamics, and so one might expect the exponents (32) to describe the semiclassical deviations of the irregular (in the sense of Percival 1973) eigenfunctions in mixed systems from their ergodic limit. (They do not describe the regular eigenfunctions, for which the corresponding moments have a different origin, and can be calculated using the results of Berry *et al.* 1983.)

4 Perturbed cat maps

We now illustrate some of the general ideas described in the previous sections by focusing on a particular example: a family of perturbed cat maps.

The maps we consider are of the form

$$\begin{pmatrix} q_{n+1} \\ p_{n+1} \end{pmatrix} = \begin{pmatrix} 2 & 1 \\ 3 & 2 \end{pmatrix} \begin{pmatrix} q_n \\ p_n \end{pmatrix} + \frac{\kappa}{2\pi} \cos(2\pi q_n) \begin{pmatrix} 1 \\ 2 \end{pmatrix} \bmod 1, \quad (33)$$

where q and p are coordinates on the unit two-torus, and are taken to be a position and its conjugate momentum. These maps are Anosov systems for $\kappa \leq \kappa_{\max} = (\sqrt{3} - 1)/\sqrt{5} \approx 0.33$; that is, for κ in this range they are completely hyperbolic and their orbits are conjugate to those of the map with $\kappa = 0$ (i.e. there are no bifurcations). Outside this range, bifurcations occur, stable islands are created, and the dynamics becomes mixed (see, for example, Berry *et al.* 1998, where these systems were used to demonstrate the influence of periodic orbit bifurcations on long-range spectral statistics).

The quantization of maps like (33) was developed by Hannay & Berry (1980), when $\kappa = 0$, and Basilio de Matos & Ozorio de Almeida (1995) for non-zero κ . The quantum kinematics associated with a phase space that has the topology of a two-torus restricts

Planck's constant to taking inverse integer values. The integer in question, N , is the dimension of the Hilbert space of admissible wavefunctions. With doubly periodic boundary conditions (see, for example, Keating *et al.* 1999), these wavefunctions in their position representation have support at points $q = Q/N$, where Q takes integer values between 1 and N . They may thus be represented by N -vectors with complex components. The quantum dynamics is then generated by an $N \times N$ unitary matrix \mathbf{U} whose action on the wavefunctions reduces to (33) in the classical limit; for example

$$U_{Q_1, Q_2} = \frac{1}{\sqrt{iN}} \exp \left[\frac{2\pi i}{N} (Q_1^2 - Q_1 Q_2 + Q_2^2) + \frac{iN}{2\pi} \kappa \sin(2\pi Q_1/N) \right]. \quad (34)$$

This matrix plays the role of the Green function of the time-dependent Shrödinger equation for flows.

Denoting the eigenvalues of \mathbf{U} by $e^{i\theta_n}$, and the corresponding eigenfunctions by $\Psi_n(Q)$, we have that

$$\sum_n |\Psi_n(Q)|^2 \delta_\varepsilon(\theta - \theta_n) = 1 + \operatorname{Re} \sum_{k=1}^{\infty} U_{Q,Q}^k \exp(-i\theta k - \varepsilon k) \quad (35)$$

where

$$\delta_\varepsilon(x) = \frac{1 - e^{-\varepsilon} \cos x}{1 + e^{-2\varepsilon} - 2e^{-\varepsilon} \cos x} \quad (36)$$

is a periodized, Lorentzian-smoothed δ -function of width ε (Keating 1991). Equation (35) is the analogue for quantum maps of (2). The left-hand side corresponds, approximately, to N times the local n -average (over a range of size of the order of ε) of $|\Psi_n(Q)|^2$, and so, dividing both sides by N and averaging smoothly with respect to Q (for example, taking the convolution with a normalized Gaussian) over a range large compared to a de Broglie wavelength ($\Delta Q = 1$) but small compared to N ,

$$\langle |\Psi_n(Q)|^2 \rangle \approx \frac{1}{N} + \frac{1}{N} \operatorname{Re} \sum_{k=1}^{\infty} \langle U_{Q,Q}^k \rangle_Q \exp(-i\theta k - \varepsilon k). \quad (37)$$

Here $\langle \dots \rangle$ denotes a combination of the n -average and the Q -average $\langle \dots \rangle_Q$.

In our computations we took ε large enough so that the dominant contributions to (35) and (37) come from the $k = 1$ terms in the sums on the right, and so, for example, we may substitute (34) directly into (37). In the semiclassical limit, as $N \rightarrow \infty$, the Q -average selects regions close to stationary points of the phase of (34), which we denote by $Q/N = q_f$. These stationary points coincide with the positions of the fixed points of the classical map (33); that is, q_f satisfies

$$q_f = \frac{1}{2} \left(j - \frac{\kappa}{2\pi} \cos(2\pi q_f) \right) \quad (38)$$

for integers j such that $0 \leq q_f < 1$ (see, for example, Boasman & Keating 1995). Expanding the phase of (34) around q_f gives, up to cubic terms,

$$U_{Q,Q} \approx \frac{1}{\sqrt{iN}} \exp \left[2\pi i S_f + \pi i N (2 - \kappa \sin(2\pi q_f)) y^2 - \frac{2\pi^2 i N}{3} \kappa \cos(2\pi q_f) y^3 \right], \quad (39)$$

where

$$y = \frac{Q}{N} - q_f \quad (40)$$

and $2\pi S_f$ denotes the phase evaluated at q_f .

Provided that $2 - \kappa \sin(2\pi q_f) \neq 0$, this approximation is dominated by the quadratic term in the exponent when y is small. It thus describes complex-Gaussian fringes around the classical fixed points with a length-scale (in terms of y) of the order of $N^{-1/2}$. These are the analogues of Bogomolny's fringes. They will be resolved if the local Q -average is over a range that is small compared to $N^{1/2}$ (but which still grows as $N \rightarrow \infty$).

For the example being considered here, when $\kappa < \kappa^* \approx 5.94338$ the two values of j in (38), $j = 0$ and $j = 1$, each give rise to a single unstable fixed point for which the condition $2 - \kappa \sin(2\pi q_f) \neq 0$ is satisfied. In Figure 1, we plot the left hand side of (35) when $\kappa = 3$, with $\varepsilon = 2.2$ and for $N = 1597$. The structure around the fixed points is clearly visible, and is most easily seen by applying the local Q -average (in this case, making a convolution with a normalized Gaussian of width 0.02).

It is at bifurcations that $2 - \kappa \sin(2\pi q_f) = 0$. Then the quadratic term in (39) vanishes, and the fringe structure comes instead from the cubic term. It thus has a y -length-scale of the order of $N^{-1/3}$. The amplitude is the same as in the case of isolated fixed points ($N^{-1/2}$ in the contribution to $\langle |\Psi_n(Q)|^2 \rangle$). In the language of Section 2, this corresponds to a codimension-one bifurcation of a periodic orbit with $r = 1$ (a tangent bifurcation).

In our example, the first bifurcation occurs when $\kappa = \kappa^*$. At this parameter value, two new degenerate solutions of (38) appear, for both $j = 0$ and $j = 1$, corresponding to the birth of a pair of fixed points, one stable and the other unstable. In Figure 2 we plot the left hand side of (35) with $\varepsilon = 2.2$ and $N = 1597$, as above, but now with $\kappa = \kappa^*$. It is apparent that the scars around the two bifurcations, at positions $q = 0.05$ and $q = 0.44$, are wider than those around the two non-bifurcating fixed points, at positions $q = 0.69$ and $q = 0.81$, and that they are also wider than those shown in Figure 1. In Figure 3 we plot the left hand side of (35) close to the bifurcation point at $q = 0.44$, together with the approximation (39), which clearly captures the details of the associated fringe structure.

It is straightforward now to deduce the semiclassical scaling with N of the moments

$$C_{2m}(N) = N^{2m} \sum_{Q=1}^N \left(\langle |\Psi_n(Q)|^2 \rangle - \frac{1}{N} \right)^{2m}. \quad (41)$$

The arguments of Section 3 suggest that C_{2m} is of the order of N^{-m+w} , where $w = 1/2$ away from bifurcations and $w = 2/3$ at the bifurcation (w is one plus the width exponents deduced from (39), because those were for y rather than Ny , as we need here). In Figure 4 we plot $\log C_2$ against $\log N$ when $\kappa = 3$. The fact that the points lie on a straight line confirms that there is a power-law scaling; furthermore, the gradient is close to $-1/2$, as expected. In Figure 5, we make the same plot for $\kappa = \kappa^*$. In this case the gradient is close to the expected value of $-1/3$ (a possible explanation for the deviation is that for the range of values of N shown, the bifurcation exponent is contaminated by the contributions

from the non-bifurcating periodic orbits). Finally, in Figure 6 we plot

$$g(m) = \lim_{N \rightarrow \infty} \frac{\log C_{2m}(N)}{\log N}, \quad (42)$$

calculated numerically from the gradients of best-fitting straight lines to plots like those in Figures 4 and 5. For both $\kappa = 3$ and $\kappa = \kappa^*$ the results are in accord with the scaling law suggested above.

We emphasize that these numerical computations illustrate the influence of one individual bifurcation only. They do not test the competition which would result from averaging over a parameter range that contains many different generic bifurcations, and which the analysis of Section 3 suggests has a universal outcome for the moment exponents.

5 Acknowledgements

It is a pleasure to acknowledge stimulating discussions with Arnd Bäcker, John Hannay and Jens Marklof, and comments on the manuscript by Sir Michael Berry. SDP wishes to thank BRIMS for financial support, and BRIMS and the School of Mathematics at the University of Bristol for hospitality during the period when this work was carried out.

References

Agam, O. & Fishman, S. 1994 Semiclassical criterion for scars in wave-functions of chaotic systems. *Phys. Rev. Lett.* **73**, 806-809.

Basílio de Matos, M. & Ozorio de Almeida, A.M. 1995 Quantization of Anosov maps. *Ann. Phys.* **237**, 46-65.

Arnold, V.I. 1978 *Mathematical Methods in Classical Mechanics*. Springer.

Bäcker, A., Schubert, R. & Stifter, P. 1998 Rate of quantum ergicity in Euclidean billiards. *Phys. Rev. E* **57**, 5425-5447.

Berry, M.V. 1977 Focusing and twinkling: critical exponents from catastrophes in non-Gaussian random short waves. *J. Phys. A* **10**, 2061-2081.

Berry, M.V. 1983 Semiclassical mechanics of regular and irregular motion. In *Les Houches Lecture Series* (ed. G. Iooss, R.H.G. Helleman & R. Stora), vol. 36, pp. 171-271 Amsterdam: North Holland.

Berry, M.V. 1989, Quantum scars of classical closed orbits in phase space. *Proc. R. Soc. Lond. A* **243**, 219-231.

Berry, M.V. 2000 Spectral twinkling. *New Directions in Quantum Chaos*. Proceedings of the International School of Physics “Enrico Fermi”, 45-63. Italian Physical Society.

Berry, M.V., Hannay, J.H. & Ozorio de Almeida, A.M. 1983 Intensity moments of semi-classical wavefunctions. *Physica D* **8**, 229-242.

Berry, M.V., Keating, J.P. & Prado, S.D. 1988 Orbit bifurcations and spectral statistics. *J. Phys. A* **31**, L245-254.

Berry, M.V., Keating, J.P. & Schomerus, H. 2000 Universal twinkling exponents for spectral fluctuations associated with mixed chaology. *Proc. R. Soc. Lond. A* **456**, 1659-1668.

Berry, M.V. & Tabor, M. 1976 Closed orbits and the regular bound spectrum. *Proc. R. Soc. Lond. A* **349**, 101-123.

Boasman, P.A. & Keating, J.P. 1995 Semiclassical asymptotics of perturbed cat maps. *Proc. R. Soc. Lond. A* **449**, 629-653.

Bogomolny, E.B. 1988 Smoothed wavefunctions of chaotic quantum systems. *Physica D* **31**, 169-189.

Colin de Verdière, Y. 1985 Ergodicité et fonctions propres du laplacien. *Commun. Math. Phys.* **102**, 497-502.

Eckhardt, B., Fishman, S., Keating, J.P., Agam, O., Main, J., & Müller, K. 1995 Approach to ergodicity in quantum wave functions. *Phys. Rev. E* **52**, 5893-5903.

Fishman, S., Georgeot, B. & Prange, R. E. 1996 Fredholm method for scars. *J. Phys. A* **29**, 919-937.

Gutzwiller, M.C. 1971 Periodic orbits and classical quantization conditions. *J. Math. Phys.* **12**, 343-358.

Gutzwiller, M.C. 1990 *Chaos in Classical and Quantum Mechanics* (New York: Springer).

Hannay, J.H. & Berry, M.V. 1980 Quantization of linear maps on the torus – Fresnel diffraction by a periodic grating. *Physica D* **1**, 267-290.

Heller, E.J. 1984 Bound state eigenfunctions of classically chaotic Hamiltonian systems - scars of periodic orbits. *Phys. Rev. Lett.* **53**, 1515-1518.

Kaplan, L. 1999 Scars in quantum chaotic wavefunctions. *Nonlinearity* **12**, R1-R40.

Keating, J.P. 1991 The cat maps: quantum mechanics and classical motion. *Nonlinearity* **4**, 309-341.

Keating, J.P., Mezzadri, F. & Robbins, J.M. 1999 Quantum boundary conditions for torus maps. *Nonlinearity* **12**, 579-591.

McDonald, S.W. 1983 *Lawrence Berkeley Laboratory Report* LBL - 14837.

Meyer, K.R. 1970 Generic bifurcations of periodic points. *Trans. Am. Math. Soc.* **149**, 95-107.

Meyer, K.R. 1986 Bibliographic notes on generic bifurcations in Hamiltonian Systems. *Contemp. Math.* **56**, 373-381.

Ozorio de Almeida, A.M. 1988 *Hamiltonian Systems: Chaos and Quantization*. Cambridge University Press.

Ozorio de Almeida, A.M. & Hannay, J.H. 1987 Resonant periodic orbits and the semi-classical energy spectrum. *J. Phys A* **20**, 5873-5883.

Percival, I.C. 1973 Regular and irregular spectra. *J. Phys. B* **6**, L229-L232.

Schomerus, H. 1998 Periodic orbits near bifurcations of codimension two: Classical mechanics, semiclassics and Stokes transitions. *J. Phys. A* **31**, 4167-4196.

Schomerus, H. & Sieber, M. 1997 Bifurcations of periodic orbits and uniform approximations. *J. Phys. A* **30**, 4537-4562.

Shnirelman, A.I. 1974 Ergodic properties of eigenfunctions (in Russian). *Usp. Math. Nauk* **29**, 181-182.

Sieber, M. 1996 Uniform approximation for bifurcations of periodic orbits with high repetition numbers. *J. Phys. A* **29**, 4715-4732.

Sieber, M. & Schomerus, H. 1998 Uniform approximations for period-quadrupling bifurcations. *J. Phys. A* **31**, 165-183.

Tomsovic, S., Grinberg, M. & Ullmo, D. 1995 Semiclassical trace formulas of near-integrable systems: Resonances. *Phys. Rev. Lett.* **75**, 4346-4349.

Ullmo, D., Grinberg, M. & Tomsovic, S. 1996 Near-integrable systems: Resonances and semiclassical trace formulas. *Phys. Rev. E* **54**, 136-152.

Zelditch, S. 1987 Uniform distribution of eigenfunctions on compact hyperbolic surfaces.
Duke Math. J. **55**, 919-941.

FIGURES

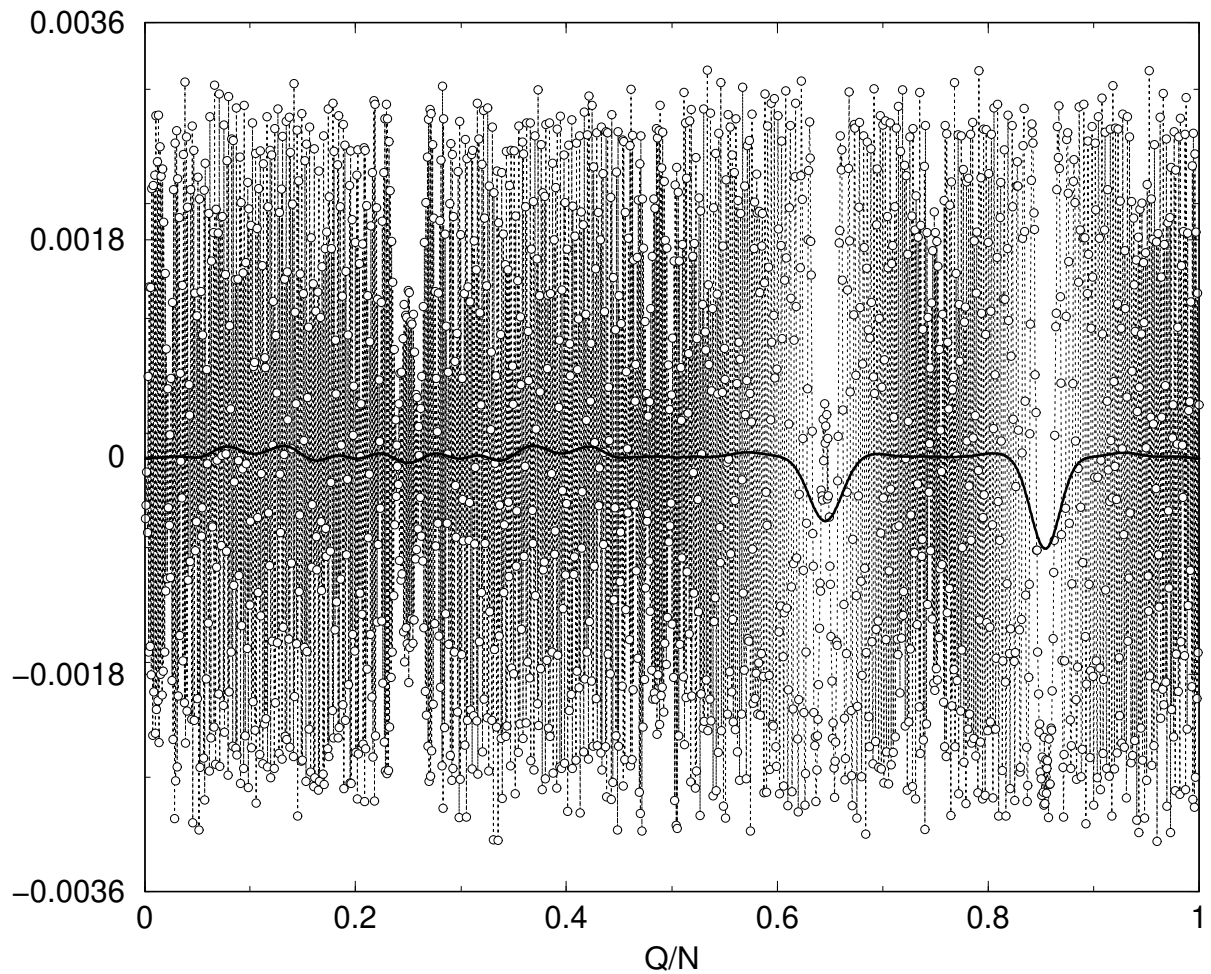


Figure 1: $\sum_n |\psi_n(Q)|^2 \delta_\varepsilon(\theta - \theta_n) - 1$, with $\varepsilon = 2.2$, $\kappa = 3$ and $N = 1597$ (circles connected by dotted lines). Also shown is a convolution of the data with a normalized Gaussian of width 0.02 (bold line). The positions of the fixed points are $q = 0.65$ and $q = 0.85$.

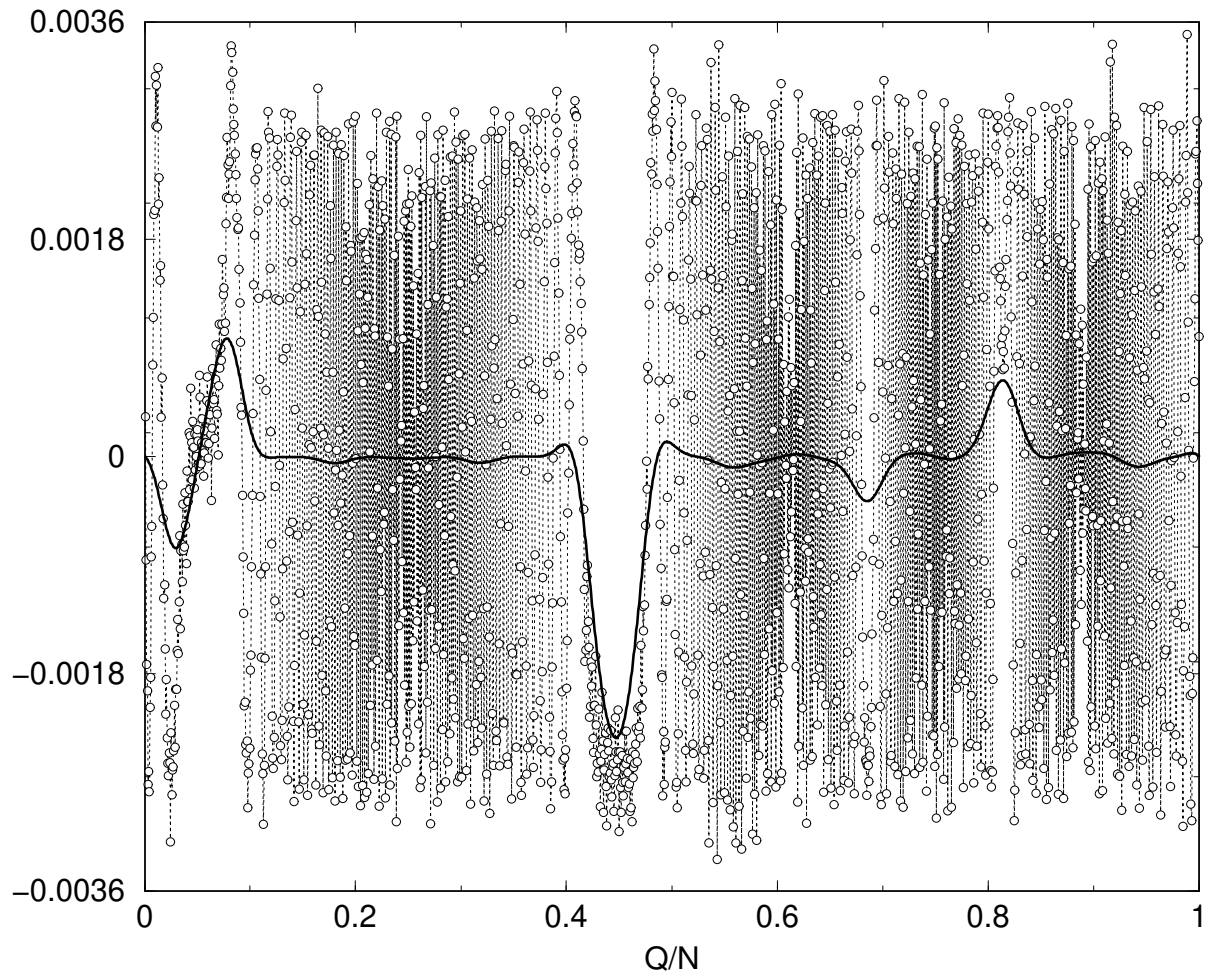


Figure 2: $\sum_n |\psi_n(Q)|^2 \delta_\varepsilon(\theta - \theta_n) - 1$, with $\varepsilon = 2.2$, $\kappa = \kappa^*$ and $N = 1597$ (circles connected by dotted lines). Also shown is a convolution of the data with a normalized Gaussian of width 0.02 (bold line). There are unstable fixed points at $q = 0.69$ and $q = 0.81$, and bifurcations at $q = 0.05$ and $q = 0.44$.

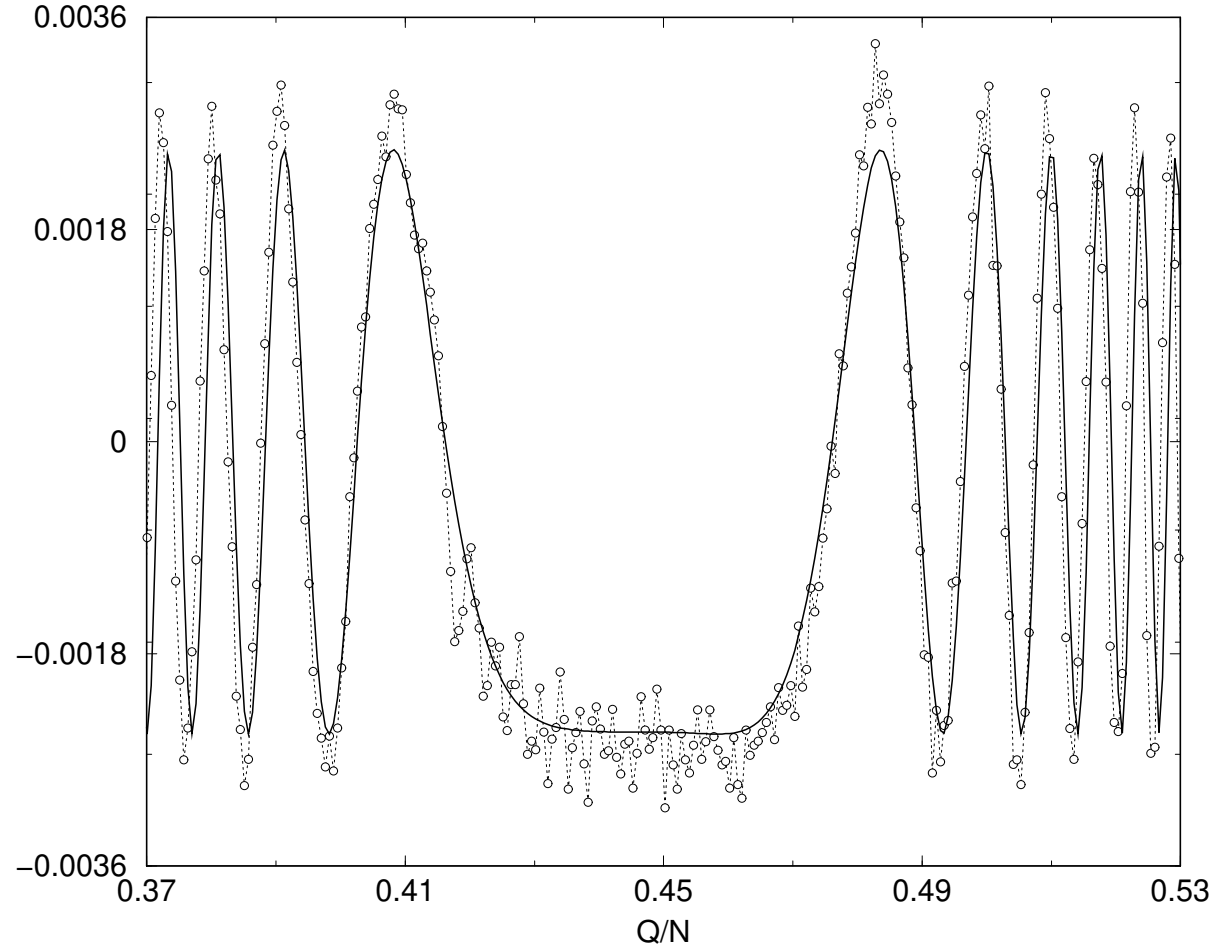


Figure 3: $\sum_n |\psi_n(Q)|^2 \delta_\varepsilon(\theta - \theta_n) - 1$, with $\varepsilon = 2.2$, $\kappa = \kappa^*$ and $N = 1597$, as in Figure 2, in the neighbourhood of the bifurcation at $q = 0.44$ (circles connected by dotted lines). Also shown is the local approximation obtained by substituting (39) into (35) (bold line).

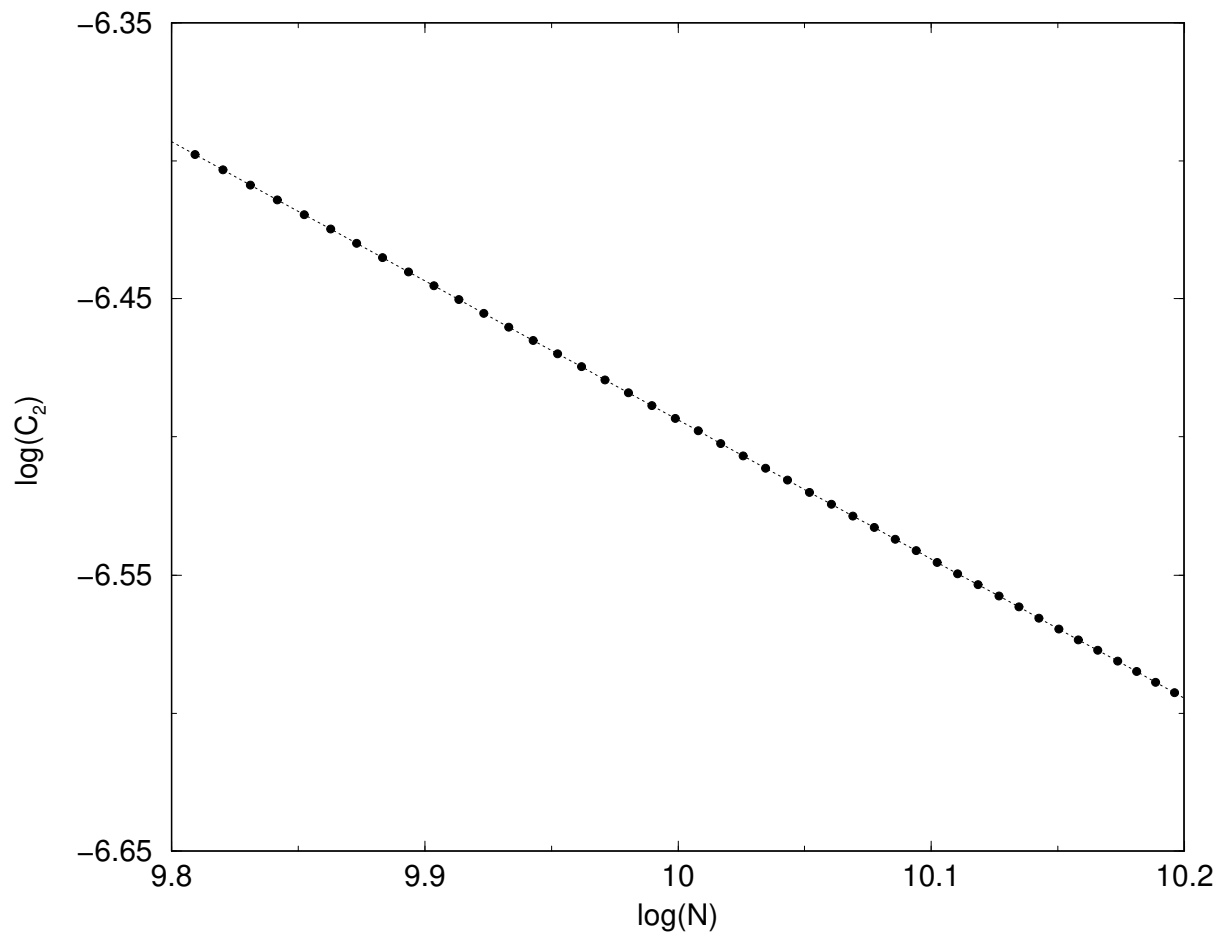


Figure 4: $\log C_2$, calculated using a local Q -average of size $0.02N^{1/2}$, plotted against $\log N$ when $\kappa = 3$ (circles). Also shown is a best-fitting straight line, which has gradient -0.50.

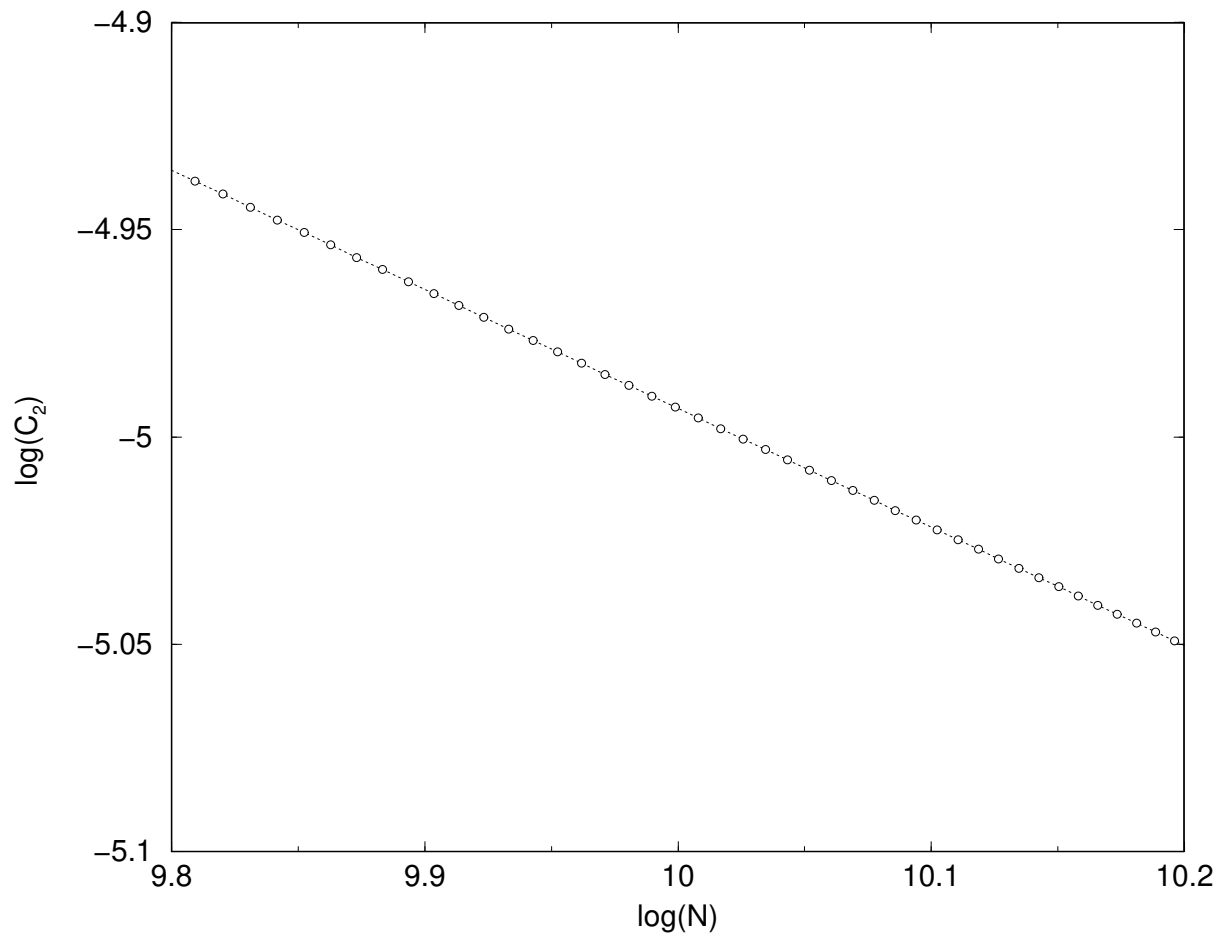


Figure 5: $\log C_2$, calculated using a local Q -average of size $0.02N^{1/2}$, plotted against $\log N$ when $\kappa = \kappa^*$ (circles). Also shown is a best-fitting straight line, which has gradient -0.29.

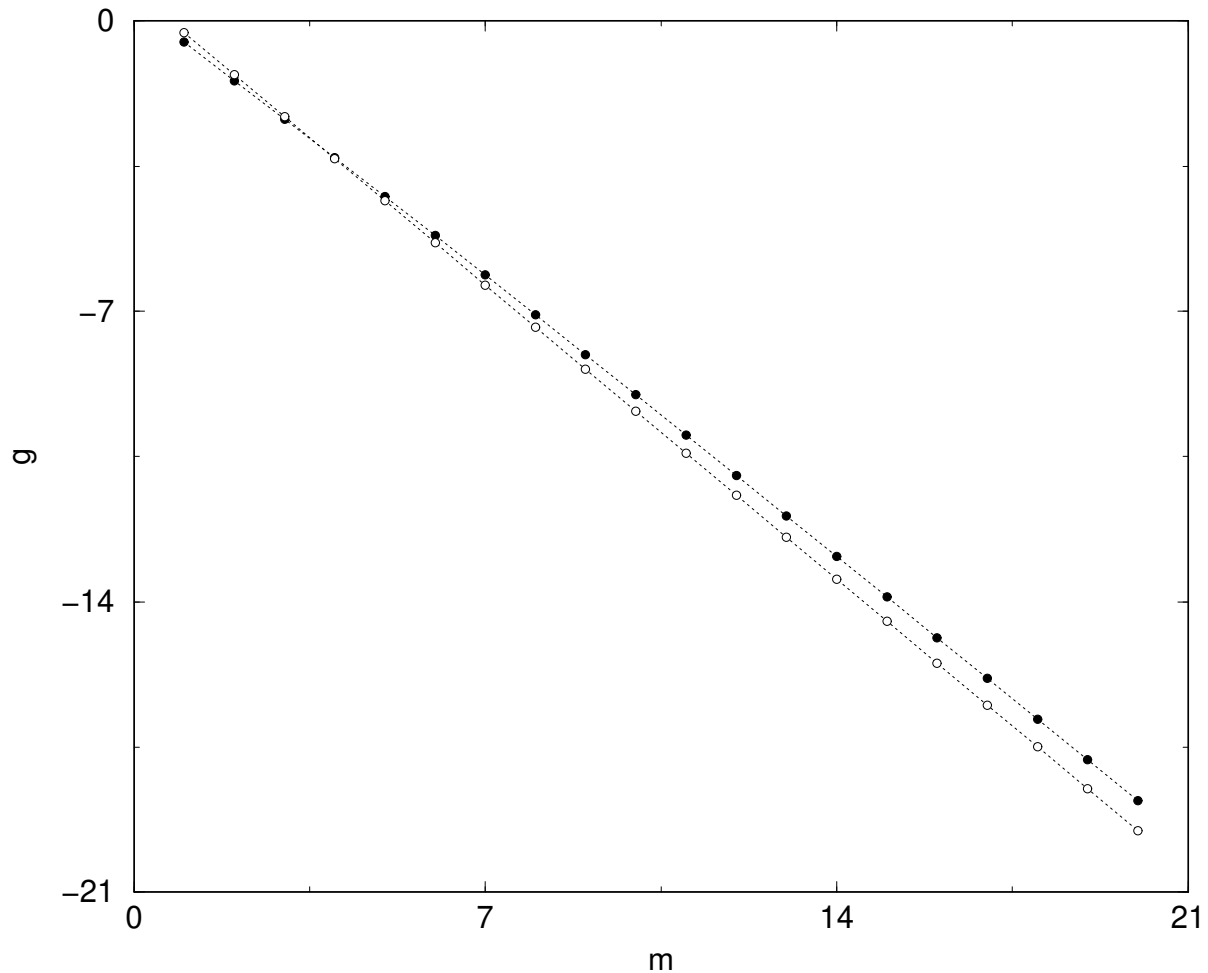


Figure 6: $g(m)$ plotted against m , for $\kappa = 3$ (full circles), and $\kappa = \kappa^*$ (open circles). Also shown are the best fitting straight lines: $g = -0.96m + 0.57$ and $g = -1.01m + 0.72$, respectively.